



# Effect of sporadic destratification, seasonal overturn, and artificial mixing on CH<sub>4</sub> emissions from a subtropical hydroelectric reservoir

Frédéric Guérin<sup>1,2,3</sup>, Chandrashekhar Deshmukh<sup>1,4,5,a</sup>, David Labat<sup>1</sup>, Sylvie Pighini<sup>6,b</sup>, Axay Vongkhamso<sup>6</sup>, Pierre Guédant<sup>6</sup>, Wanidaporn Rode<sup>6</sup>, Arnaud Godon<sup>6,c</sup>, Vincent Chanudet<sup>7</sup>, Stéphane Descloux<sup>7</sup>, and Dominique Serça<sup>4</sup>

<sup>1</sup>Université de Toulouse, UPS GET, 14 Avenue E. Belin, 31400 Toulouse, France

<sup>2</sup>IRD, UR 234, GET, 14 Avenue E. Belin, 31400 Toulouse, France

<sup>3</sup>Departamento de Geoquímica, Universidade Federal Fluminense, Niteroi-RJ, Brazil

<sup>4</sup>Laboratoire d'Aérodologie, Université de Toulouse, CNRS UMR 5560; 14 Av. Edouard Belin, 31400 Toulouse, France

<sup>5</sup>Centre for Regulatory and Policy Research, TERI University, New Delhi, India

<sup>6</sup>Nam Theun 2 Power Company Limited (NTPC), Environment & Social Division, Water Quality and Biodiversity Dept., Gnommalath Office, P.O. Box 5862, Vientiane, Lao PDR

<sup>7</sup>Electricité de France, Hydro Engineering Centre, Sustainable Development Dpt., Savoie Technolac, 73373 Le Bourget du Lac, France

<sup>a</sup>now at: Nam Theun 2 Power Company Limited (NTPC), Environment & Social Division, Water Quality and Biodiversity Dept., Gnommalath Office, P.O. Box 5862, Vientiane, Lao PDR

<sup>b</sup>now at: Innsbruck University, Institute of Ecology, 15 Sternwartestrasse, 6020 Innsbruck, Austria and Foundation Edmund Mach, FOXLAB-FEM, Via E. Mach 1, 38010 San Michele all'Adige, Italy

<sup>c</sup>now at: Arnaud Godon Company, 44 Route de Genas, Nomade Lyon, 69003 Lyon, France

*Correspondence to:* Frédéric Guérin (frederic.guerin@ird.fr)

Received: 5 June 2015 – Published in Biogeosciences Discuss.: 20 July 2015

Revised: 30 May 2016 – Accepted: 1 June 2016 – Published: 22 June 2016

**Abstract.** Inland waters in general and freshwater reservoirs specifically are recognized as a source of CH<sub>4</sub> into the atmosphere. Although the diffusion at the air–water interface is the most studied pathway, its spatial and temporal variations are poorly documented.

We measured temperature and O<sub>2</sub> and CH<sub>4</sub> concentrations every 2 weeks for 3.5 years at nine stations in a subtropical monomictic reservoir which was flooded in 2008 (Nam Theun 2 Reservoir, Lao PDR). Based on these results, we quantified CH<sub>4</sub> storage in the water column and diffusive fluxes from June 2009 to December 2012. We compared diffusive emissions with ebullition from Deshmukh et al. (2014) and aerobic methane oxidation and downstream emissions from Deshmukh et al. (2016).

In this monomictic reservoir, the seasonal variations of CH<sub>4</sub> concentration and storage were highly dependent on

the thermal stratification. Hypolimnetic CH<sub>4</sub> concentration and CH<sub>4</sub> storage reached their maximum in the warm dry season (WD) when the reservoir was stratified. Concentration and storage decreased during the warm wet (WW) season and reached its minimum after the reservoir overturned in the cool dry (CD) season. The sharp decreases in CH<sub>4</sub> storage were concomitant with extreme diffusive fluxes (up to 200 mmol m<sup>-2</sup> d<sup>-1</sup>). These sporadic emissions occurred mostly in the inflow region in the WW season and during overturn in the CD season in the area of the reservoir that has the highest CH<sub>4</sub> storage. Although they corresponded to less than 10 % of the observations, these extreme CH<sub>4</sub> emissions (> 5 mmol m<sup>-2</sup> d<sup>-1</sup>) contributed up to 50 % of total annual emissions by diffusion.

During the transition between the WD and WW seasons, a new emission hotspot was identified upstream of the water

intake where diffusive fluxes peaked at  $600 \text{ mmol m}^{-2} \text{ d}^{-1}$  in 2010 down to  $200 \text{ mmol m}^{-2} \text{ d}^{-1}$  in 2012. The hotspot was attributed to the mixing induced by the water intakes (artificial mixing). Emissions from this area contributed 15–25 % to total annual emissions, although they occur in a surface area representative of less than 1 % of the total reservoir surface. We highly recommend measurements of diffusive fluxes around water intakes in order to evaluate whether such results can be generalized.

## 1 Introduction

Since the 1990s, hydroelectric reservoirs are known to be a source of methane (CH<sub>4</sub>) into the atmosphere. Their contribution to total CH<sub>4</sub> emissions still needs refinement since the discrepancies among estimates is large, ranging from 1 to 12 % of total CH<sub>4</sub> emissions (St Louis et al., 2000; Barros et al., 2011). These two estimates are mostly based on diffusive fluxes at the air–water interface, and they overlook emissions from the rivers downstream of the dams (Abril et al., 2005; Guérin et al., 2006; Kemenes et al., 2007; Teodoru et al., 2012; Maeck et al., 2013; Deshmukh et al., 2016), CH<sub>4</sub> ebullition (DelSontro et al., 2010; Deshmukh et al., 2014) and emissions from the drawdown area of reservoirs (Chen et al., 2009, 2011), although these pathways could largely dominate diffusion at the surface of the reservoirs.

Even if CH<sub>4</sub> diffusion at the surface of a reservoir is the best-documented emission pathway, little information is available on spatial and temporal variability of CH<sub>4</sub> emissions by diffusive fluxes. In tropical amictic and well-stratified reservoirs with CH<sub>4</sub>-rich hypolimnion, the highest diffusive fluxes are usually observed during dry periods and when the stratification weakens at the beginning of the rainy season (Guérin and Abril, 2007). A study of CH<sub>4</sub> emissions from a dimictic reservoir suggests a potential large outgassing of CH<sub>4</sub> during the overturn (Utsumi et al., 1998b), as is the case in natural monomictic and dimictic lakes (Kankaala et al., 2007; López Bellido et al., 2009; Schubert et al., 2010; Schubert et al., 2012; Fernández et al., 2014). Such hot moments of emissions (McClain et al., 2003) could contribute 45–80 % of annual CH<sub>4</sub> emissions by diffusion (Schubert et al., 2012; Fernández et al., 2014). They are rarely taken into account in carbon budgets since they can only be captured by high-frequency monitoring. Spatial heterogeneity of CH<sub>4</sub> emissions at the surfaces of reservoirs is also very high. It mostly depends on the spatial variations of ebullition that is controlled by sedimentation (DelSontro et al., 2011; Sobek et al., 2012; Maeck et al., 2013). The spatial variability of diffusion in reservoirs is less prominent, with a few exceptions of higher emissions (1) in areas where dense forest is flooded (Abril et al., 2005), (2) at shallow sites (< 10 m) (Zheng et al., 2011; Sturm et al., 2014), and (3) at river inflows (Musenze et al., 2014). However, as was shown

for CO<sub>2</sub> emissions from a tropical hydroelectric reservoir, taking into account both spatial and temporal variability of emissions significantly affects positively or negatively carbon budgets and emission factors (Pacheco et al., 2015).

In the framework of a comprehensive project aiming at quantifying greenhouse gas emissions from the Nam Theun 2 Reservoir (NT2R), a recently flooded subtropical reservoir located in the Lao People's Democratic Republic (PDR), we studied (1) the spatial and temporal variability of CH<sub>4</sub> ebullitive fluxes (Deshmukh et al., 2014) and (2) the downstream CH<sub>4</sub> emissions (Deshmukh et al., 2016). In the present study, the objective is to quantify the CH<sub>4</sub> diffusive fluxes at the surface of the NT2R and evaluate the significance of the diffusive fluxes in total methane emissions in a subtropical monomictic reservoir with a peculiar water intake that artificially mixes the water column. The CH<sub>4</sub> emissions were quantified every 2 weeks during 3.5 years (June 2009 to December 2012) based on a monitoring of CH<sub>4</sub> concentrations in the reservoir water column. This was performed at nine stations flooding different types of ecosystems. On the basis of these results, we discuss the spatial and temporal variations of the CH<sub>4</sub> emissions by diffusive fluxes and the significance of hotspots and hot moments in the total emissions from the surface of the reservoir.

## 2 Material and methods

### 2.1 Study area

The NT2 hydroelectric reservoir ( $17^{\circ}59'49'' \text{ N}$ ,  $104^{\circ}57'08'' \text{ E}$ ) was built on the Nam Theun River located in the subtropical region of Lao PDR on the Nakai Plateau. A detailed description of this trans-basin hydroelectric reservoir located on the Nakai Plateau is given in Descloux et al. (2016). Basically, the Nam Theun River is dammed (Nakai Dam, ND in Fig. 1) and the water from the Nam Theun River is diverted to the Xebang Fai watershed after passing through water intake (WI in Fig. 1) to the powerhouse (PH in Fig. 1). The WI is located in a 130 m wide and 9–20 m deep channel on the south-western side of the reservoir, and it is located 5 m above the bottom (in Supplement Fig. S1). The powerhouse is located in the valley 200 m below the plateau. The filling of the reservoir began in April 2008, with full water level reached by October 2009 and the power plant commissioned in April 2010. After that date, turbines were turned on and water was continuously delivered to the turbines and downstream of the reservoir. Annually, the NT2R receives around  $7527 \text{ Mm}^3$  of water from the Nam Theun watershed, which is more than twice the volume of the reservoir ( $3908 \text{ Mm}^3$ ). A continuous flow of  $2 \text{ m}^3 \text{ s}^{-1}$  (and occasionally spillway release) is discharged from the Nakai Dam (ND in Fig. 1) to the Nam Theun River. This low water discharge corresponds to the minimum water discharge of the Nam Theun River before the dam was built.

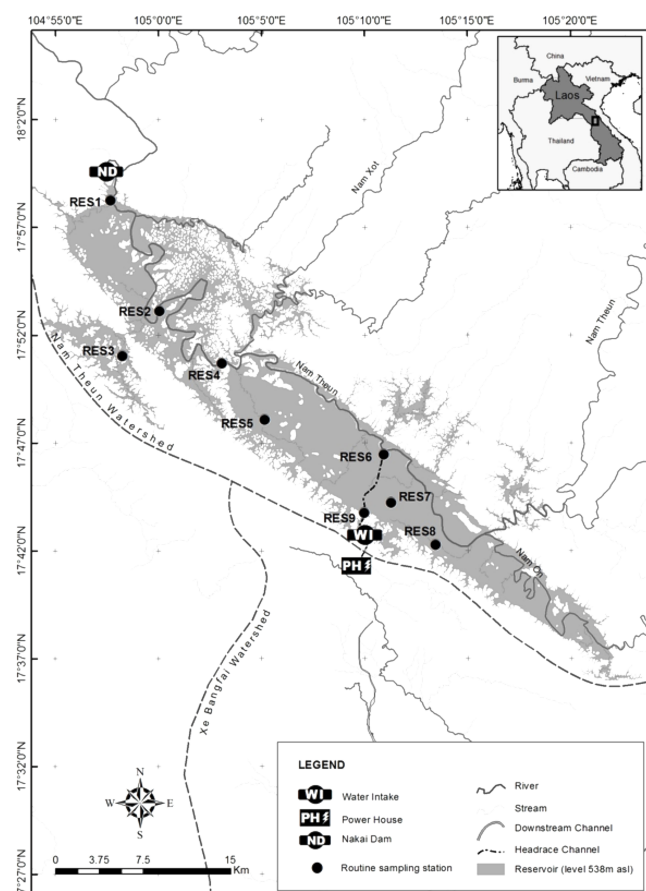


**Figure 1.** Map of the sampling stations and civil structures at the Nam Theun 2 Reservoir (Lao PDR).

Typical meteorological years are characterized by three seasons: warm wet (WW) (mid-June–mid-October), cool dry (CD) (mid-October–mid-February), and warm dry (WD) (mid-February–mid-June). Daily air temperature varies between 14 °C (CD season) and 30 °C (WD season). The mean annual rainfall is about 2400 mm and occurs mainly (80 %) in the WW season.

During the filling of the reservoir, 489 km<sup>2</sup> of soils and different types of vegetation (Descloux et al., 2011) were flooded by the end of October 2008. The water level in the reservoir was nearly constant from October 2009 to April 2010 (Fig. 2a). After the commissioning (from April 2010 to December 2012) the reservoir surface varied seasonally by a factor of 3 and reached its maxima (489 km<sup>2</sup>) and minima (168 to 176 km<sup>2</sup>, depending on the years) during the WW and WD seasons, respectively (Fig. 2a). The average water volume is 2.65 km<sup>3</sup>, with the lowest volume by the end of the WD season (0.71 in June 2011) and the highest at the end of the rainy seasons (3.97 km<sup>3</sup> in September 2011) (Fig. 2b). The seasonal water level variations are about 10 m (Fig. 2c); the average depth is 8 m for a maximum depth of 39 m close to the Nakai Dam.

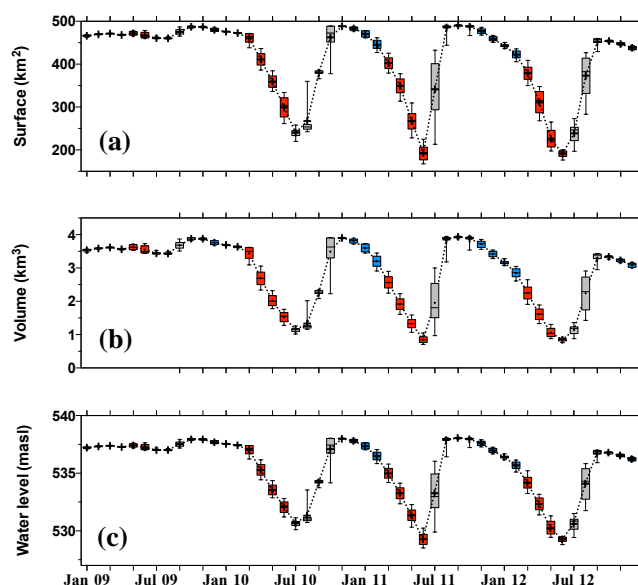


**Figure 2.** Variations of (a) surface of the reservoir (km<sup>2</sup>), volume of water (km<sup>3</sup>), and water level (m a.s.l.) at the Nam Theun 2 Reservoir between January 2009 and December 2012.

## 2.2 Sampling strategy

A total of nine stations (RES1–9, Fig. 1) located in the reservoir were monitored every 2 weeks (fortnightly) in order to determine the vertical profiles of temperature and O<sub>2</sub> and CH<sub>4</sub> concentrations in the water column. The type of ecosystems flooded, the depth range, and the hydrology of the stations are given in Table 1. Basically, three stations are located on the thalweg of the former Nam Theun River (RES2, RES4, RES6), whereas four other stations are located in a small embayment in the flooded dense forest (RES3), flooded degraded forest (RES5), flooded swamp area (RES7), and flooded agricultural land (RES8). The RES1 station is located 100 m upstream of the Nakai Dam, and the RES9 station is located 800 m upstream of the water intake (WI) delivering the water to the powerhouse (Figs. 1 and S1). Station RES9 is under the influence of the water column mixing induced by the water withdrawal at the WI, located at the bottom of the reservoir (5 m above the bottom) and under 10 to 20 m of water (see discussion). All samples and in situ measurements were taken in the morning or early afternoon from an anchored boat. Most of the time, the boat was attached to a buoy at the sampling station. When no buoy was present, an anchor was used with care in order not to re-suspend surface sediments. As the sampling started from the surface, the bottom water was sampled almost an hour later and should not be influenced by the perturbation generated by the anchor.

**Table 1.** Characteristics of the nine monitoring stations in the Nam Theun 2 Reservoir.

Station	Depth (min–max) (m)	Flooded ecosystem <sup>1</sup>	Hydrology	Water residence time index <sup>2</sup>
RES1	25.4–35	Dense forest	100 m upstream of the Nakai Dam	4
RES2	18.4–28	Dense forest	Thalweg of the Nam Theun River	4
RES3	6.4–16	Dense forest	Embayment	3
RES4	17.4–27	Degraded forest	Confluence: Nam Theun and Nam Xot Rivers	4
RES5	8.4–18	Degraded forest	Aside from the main stream	4
RES6	15.4–25	Degraded forest	Thalweg of the Nam Theun River	5
RES7	5.4–15	Swamp	Between inflows and water intake	5
RES8	11.4–21	Agricultural soils	Between inflows and water intake	5
RES9	9.4–19	Civil construction	Water intake	5

<sup>1</sup> Descloux et al. (2011). <sup>2</sup> Water renewal index in arbitrary units; <sup>3</sup> stands for longer residence time, <sup>4</sup> for average residence times and <sup>5</sup> for shorter residence times than average for the whole reservoir.

## 2.3 Experimental methods

### 2.3.1 Vertical profiles of oxygen and temperature

Vertical profiles of O<sub>2</sub> and temperature have been measured in situ at all sampling stations with a Quanta<sup>®</sup> multi-parameter probe (Hydrolab, Austin, Texas) since June 2009. In the reservoir, the vertical resolution was 0.5 m above the oxic–anoxic limit and 1 to 5 m in the hypolimnion.

### 2.3.2 Methane concentration in water

The evolution of CH<sub>4</sub> concentrations has been monitored every 2 weeks from May 2009 to December 2012. Surface samples were taken with a surface custom-built water sampler (Abril et al., 2007). Other samples from the water column were taken with an Uwitac water sampler at 3 m depth, at the oxic–anoxic interface 1 m above and below the oxic–anoxic interface and every 3 to 5 m down to 0.5 m above the bottom. Water samples were stored without air bubbles in serum glass vials, capped with butyl stoppers, sealed with aluminium crimps, and preserved with HgCl<sub>2</sub> (Guérin and Abril, 2007). Samples were analysed within 15 days. Before gas chromatography analysis for CH<sub>4</sub> concentration, a N<sub>2</sub> headspace was created and the vials were vigorously shaken to ensure an equilibration between the liquid and gas phases. The concentration in the water was calculated using the solubility coefficient of Yamamoto et al. (1976).

### 2.3.3 Gas chromatography

Analysis of CH<sub>4</sub> concentrations was performed by gas chromatography (SRI 8610C gas chromatograph, Torrance, CA, USA) equipped with a flame ionization detector. A subsample of 0.5 mL from the headspace of water sample vials was injected. Commercial gas standards (10, 100, and 1010 ppmv, Air Liquid “crystal” standards) were injected after analysis of every 10 samples for calibration. Duplicate injection of samples showed reproducibility better than 5 %.

### 2.3.4 Water column CH<sub>4</sub> storage

Between sampling depths of the vertical CH<sub>4</sub> profiles, concentrations were assumed to change linearly in order to calculate the concentration in each 1 m layer of water. The volume of water in each layer was calculated using the volume-capacity curve (NTPC, 2005). The CH<sub>4</sub> storage was calculated by multiplying the average CH<sub>4</sub> concentrations of each layer by the volume of the layer and summing up the amount of CH<sub>4</sub> for all depth intervals.

### 2.3.5 Aerobic CH<sub>4</sub> oxidation

The depth-integrated CH<sub>4</sub> oxidation rates at each station were calculated on the basis of the specific oxidation rates (d<sup>-1</sup>) determined at the NT2R (Deshmukh et al., 2016) and vertical CH<sub>4</sub> and O<sub>2</sub> profiles in the water column as already described in Guérin and Abril (2007). The depth-integrated CH<sub>4</sub> oxidation rates at each station were estimated only from January 2010 since the vertical resolution of the vertical profiles of O<sub>2</sub> and CH<sub>4</sub> was not high enough in 2009.

As the aerobic methane oxidation rates we obtained were potential, CH<sub>4-ox</sub> were corrected for two limiting factors, the oxygen availability and the light inhibition as described in Guérin and Abril (2007). The final equation to compute in situ oxidation rates (CH<sub>4-ox</sub>, mmol m<sup>-2</sup> d<sup>-1</sup>) is

$$\text{CH}_{4\text{-ox}} = C_{\text{CH}_4} \cdot S_{\text{CH}_4\text{-ox}} \cdot C_{\text{O}_2} / (C_{\text{O}_2} + K_{m(\text{O}_2)}) \cdot d \cdot I(z),$$

with  $C_{\text{CH}_4}$  the CH<sub>4</sub> concentration,  $S_{\text{CH}_4\text{-ox}}$  the specific CH<sub>4-ox</sub> from Deshmukh et al. (2016),  $C_{\text{O}_2}$  the oxygen concentration,  $K_{m(\text{O}_2)}$  the half-saturation constant ( $K_m$ ) of O<sub>2</sub> for CH<sub>4</sub> oxidation,  $d$  depth of the water layer, and  $I(z)$  the inhibition of methanotrophic activity by light as defined by Dumestre et al. (1999) at the Petit Saut Reservoir. Finally, the CH<sub>4</sub> oxidation rates were integrated in the oxic water column, from the water surface to the limit of oxygen penetration.

## 2.4 Diffusive fluxes from surface concentrations

The diffusive CH<sub>4</sub> fluxes were calculated from the monitoring of surface concentrations with the thin boundary layer (TBL) equation at all stations in the reservoir (RES1–9). The CH<sub>4</sub> surface concentrations in water and the average CH<sub>4</sub> concentration in air (1.9 ppmv) obtained during eddy covariance deployments (Deshmukh et al., 2014) were applied in Eq. (1) to calculate diffusive flux:

$$F = k_T \times \Delta C, \quad (1)$$

where  $F$ , the diffusive flux at the water–air interface;  $\Delta C = C_w - C_a$ , the concentration gradient between the water ( $C_w$ ) and the concentration at equilibrium with the overlying atmosphere ( $C_a$ ) and  $k_T$ , the gas transfer velocity at a given temperature ( $T$ ):

$$k_T = k_{600} \times (600/Sc_T)^n, \quad (2)$$

with  $Sc_T$  the Schmidt number of CH<sub>4</sub> at a given temperature ( $T$ ) (Wanninkhof, 1992) and  $n$  a number that is either 2/3 for low wind speed ( $< 3.7 \text{ m s}^{-1}$ ) or 1/2 for higher wind speed and turbulent water (Jahne et al., 1987).

For the determination of  $k_{600}$  at stations RES1–8, we averaged the formulations from Guérin et al. (2007) which include the cumulative effect of wind ( $U_{10}$ ) and rain ( $R$ ) on  $k_{600}$  ( $k_{600} = 1 : 66e^{0.26U_{10}} + 0 : 66R$ ), and the formulation of MacIntyre et al. (2010) ( $k_{600} = 2.25 U_{10} + 0.16$ ) whatever the buoyancy fluxes. As shown by Deshmukh et al. (2014), the average of the fluxes obtained from these two relationships compared well with fluxes measured by floating chambers at the reservoir surface during three deployments at the NT2R. Since the water current velocities were lower than  $1 \text{ cm s}^{-1}$  in most of the reservoir (Chanudet et al., 2012), the effect of water current on  $k_{600}$  was not included. The average wind speed (at 10 m height) and rainfall from two meteorological stations located at the Ban Thalang Bridge (close to the RES4 station) and close to the WI (Fig. 1) was used for the calculation of fluxes of all stations (RES1–8). On average for all stations and all sampling dates, the  $k_{600}$  was  $5.6 \pm 5.3 \text{ cm h}^{-1}$ , ranging from  $0.91$  to  $40.4 \text{ cm h}^{-1}$ . The lowest  $k_{600}$  were calculated in the CD season ( $3.43 \pm 1.01 \text{ cm h}^{-1}$ ;  $1.65$ – $6.06 \text{ cm h}^{-1}$ ), while the highest were obtained during the WW season ( $6.78 \pm 6.33 \text{ cm h}^{-1}$ ;  $1.57$ – $40.42 \text{ cm h}^{-1}$ ) due to high rainfall (up to  $113 \text{ mm day}^{-1}$ ). In the WD season  $k_{600}$  averaged  $5.58 \pm 4.81 \text{ cm h}^{-1}$ . This average  $k_{600}$  is significantly enhanced by some rainy events in late May–early June in 2010 and 2012 (up to  $60 \text{ mm d}^{-1}$ ).

At the water intake (RES9) where the hydrology and hydrodynamics are different from the other stations, it was impossible to quantify the  $k_{600}$  since the boat drifted quickly to the shoreline because of water currents in the narrow channel (Fig. S1). According to Chanudet et al. (2012), water current velocity in this area of the reservoir is about  $0.2 \text{ m s}^{-1}$ . Af-

ter Borges et al. (2004), the contribution of such water currents in a water body with depths ranging from 9 to 20 m is  $2.0 \pm 0.5 \text{ cm h}^{-1}$ , which should be summed up with the contribution of wind and rainfall from Guérin et al. (2007) and MacIntyre et al. (2010). It gives an average of  $9 \text{ cm h}^{-1}$ . The  $k_{600}$  was determined in the regulating dam located downstream of the turbine where we visually observed vortexes similar to those observed at RES9. In the regulating dam, the  $k_{600}$  obtained in May 2009 and March 2010 with a drifting floating chamber as described in Deshmukh et al. (2014) was  $19 \text{ cm h}^{-1}$  on average for four measurements ranging from 9 to  $40 \text{ cm h}^{-1}$ . In order to be conservative for the estimation of emissions from the water intake, we considered a constant value of  $k_{600}$  ( $10 \text{ cm h}^{-1}$ ), which is in the lower range of (1) the  $k_{600}$  calculated from Guérin et al. (2007), MacIntyre et al. (2010), and Borges et al. (2004), and (2)  $k_{600}$  values determined in the regulating dam that we consider an area with comparable hydrology/hydrodynamics.

## 2.5 Total emissions by diffusive fluxes

Based on physical modelling (Chanudet et al., 2012), it has been shown that station RES9 located at the water intake is representative of an area of  $\sim 3 \text{ km}^2$  (i.e. 0.6 % of the reservoir water surface), whatever the season. This  $3 \text{ km}^2$  area was used to extrapolate specific diffusive fluxes from RES9. The embayment where RES3 is located represents a surface area of 5–6 % of the total surface area of the reservoir, whatever the season (maximum  $28 \text{ km}^2$ ), to which were attributed the specific diffusive fluxes from RES3. The diffusive fluxes calculated for the RES1, RES2, RES4, RES5, RES6, RES7, and RES8 stations were attributed to the water surface area representative of each station, taking into account the seasonal variation of the reservoir water surface from the surface-capacity curve (NTPC, 2005).

## 2.6 Statistical and correlation analysis

Statistical tests were performed to assess the spatial and temporal variations in the surface CH<sub>4</sub> concentrations and diffusive fluxes at all stations in the reservoir. Normality of the concentration and diffusive data sets was tested with R software (R Development Core Team, 2008) and the Nortest package (Gross and Ligges, 2015). The data distribution was tested with the Fitdistrplus package (Delignette-Muller et al., 2015).

Since all tests indicated that the distribution of the data was neither normal nor lognormal, Kruskal–Wallis and Mann–Whitney tests were performed with GraphPad Prism (GraphPad Software, Inc., v5.04). No significant differences were found between the seasons and/or the stations. These test results were attributed to the very large range of surface concentrations due to the sporadic occurrence of extreme values (over 4 orders of magnitude). In order to reduce this range, the log of the concentrations was used. For each station, the

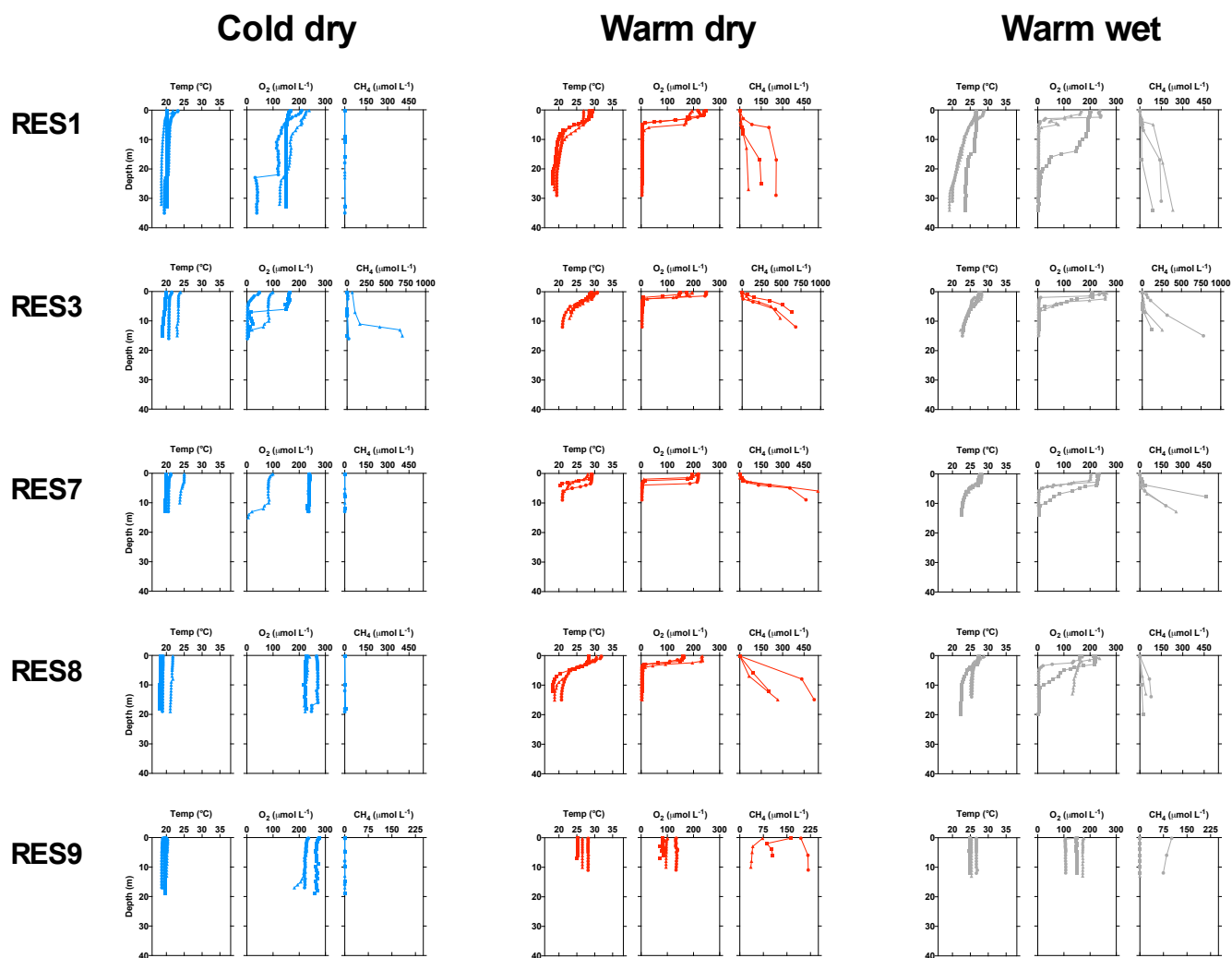


**Figure 3.** Vertical profiles of temperature ( $^{\circ}\text{C}$ ), oxygen ( $\mu\text{mol L}^{-1}$ ), and methane ( $\mu\text{mol L}^{-1}$ ) at stations RES1, RES3, RES7, RES8, and RES9 in the Nam Theun 2 Reservoir. Representative profile of the years 2010 (circle), 2011 (square), and 2012 (triangle) are given for each season: cool dry in blue, warm dry in red, and warm wet in grey. Note that for stations RES3 and RES9, the scale is different for the vertical profiles of CH<sub>4</sub>.

time series of the log of the CH<sub>4</sub> surface concentrations were linearly interpolated and re-sampled every 15 days in order to compare time series with the same number of observations. The log of the concentrations was used to determine the frequency distribution, the skewness of the data set (third-order moment), the auto-correlation of each time series, and the correlation between the different stations. All analyses were performed using Matlab.

### 3 Results

#### 3.1 Temperature and O<sub>2</sub> dynamics in the reservoir

During the 3.5 years of monitoring at stations RES1–8, the NT2R was thermally stratified with a thermocline at  $4.5 \pm 2.6$  m depth in the WD (February–June) season as re-

vealed by the vertical profiles of temperature (Fig. 3). In the WW season, the temperature vertical profiles at stations RES1–8 showed a thermocline (RES7 and RES8 in 2010 and 2011, Fig. 3), whereas on some occasions, the temperature decreased regularly from the surface to the bottom during sporadic destratification (RES1–3, Fig. 3). On average during the WW season, a thermocline was located at  $5.8 \pm 4.8$  m depth. During the CD season, the reservoir overturned as already mentioned by Chanudet et al. (2012) and the temperature was constant from the surface to the bottom (Fig. 3) in the different years. In order to illustrate the destratification, a stratification index ( $\Delta T$ ) which corresponds to the difference between the surface and bottom water temperature was defined (Fig. 4a). During the periods of stratification in the WD seasons,  $\Delta T$  was up to  $10^{\circ}\text{C}$  higher than during reservoir overturn in the CD season, with  $\Delta T$  close to zero (Fig. 4a).

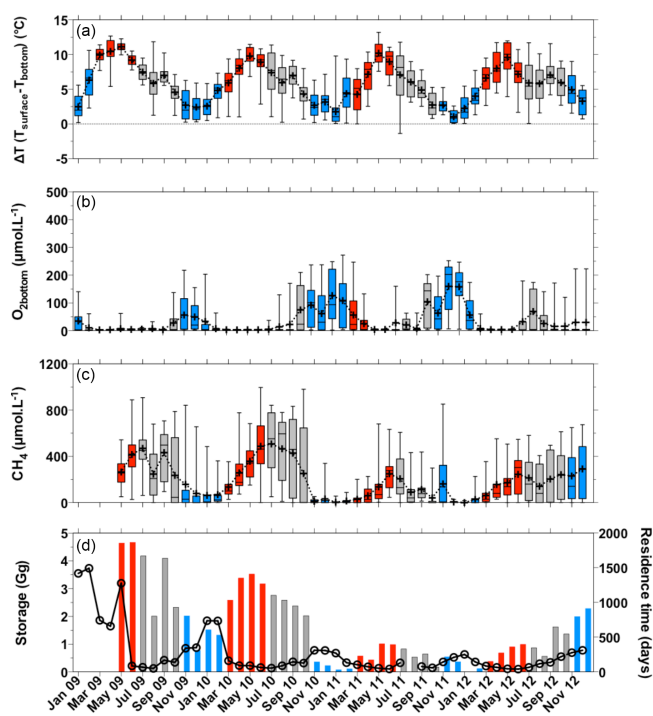


**Figure 4.** (a) Stratification index ( $\Delta T$ , see text), (b) O<sub>2</sub> concentration in the hypolimnion ( $\mu\text{mol L}^{-1}$ ), (c) CH<sub>4</sub> concentration in the hypolimnion ( $\mu\text{mol L}^{-1}$ ), and (d) CH<sub>4</sub> storage in the water column ( $\text{Gg}(\text{CH}_4) \text{ month}^{-1}$ , bars) and water residence time (days, black line with circles) in the Nam Theun 2 Reservoir (Lao PDR) between 2009 and 2012. The red, grey, and blue colours indicate the warm dry (WD), warm wet (WW), and cool dry (CD) seasons, respectively. For panels (a), (b), and (c), the boxes show the median and the interquartile range, the whiskers denote the full range of values, and the plus sign (+) denotes the mean.

During the WW season, the  $\Delta T$  decreased gradually, which means that the overturn occurred over several months.

During the WD season at the stations RES1–8, an oxycline was most of the time located at a depth concomitant with the depth of the thermocline, whereas oxygen penetrated deeper in the WW season (Fig. 3). During these two seasons, the epilimnion was always well oxygenated, with O<sub>2</sub> concentrations higher than  $200 \mu\text{mol L}^{-1}$ . In the WD season, the hypolimnion was completely anoxic, whereas O<sub>2</sub> reached occasionally the hypolimnion during the sporadic destratification events in the WW season ( $29 \pm 54 \mu\text{mol L}^{-1}$ , Figs. 3 and 4b). During the CD season (reservoir overturn), the water column was often oxygenated from the top to the bottom of the reservoir (Fig. 3). On average over the whole reservoir, the lowest hypolimnetic oxygen concentration was observed in 2010 before the reservoir was commissioned (Fig. 4b).

After the commissioning of the reservoir and the turbines were powered on in April 2010, the water column located near the intake (RES9) completely mixed, as indicated by the homogeneous temperature and oxygen profiles with depth in

every season (Fig. 3). The water column at RES9 was always well oxygenated ( $163 \pm 62 \mu\text{mol L}^{-1}$ , Fig. 3).

### 3.2 Seasonal dynamics of the CH<sub>4</sub> concentration in the reservoir

At stations RES1–8, when the water column is thermally stratified with a steep oxycline in the WD and often in the WW seasons, CH<sub>4</sub> concentrations are on average  $\sim 150$  times higher in the reservoir hypolimnion ( $246 \pm 234 \mu\text{mol L}^{-1}$ ) than in the epilimnion ( $1.6 \pm 7.7 \mu\text{mol L}^{-1}$ ) (Fig. 3). The gradient of CH<sub>4</sub> concentration at the thermocline/oxycline was steeper during the WD season than during the WW season (Fig. 3). During the CD season, the average CH<sub>4</sub> concentration in the reservoir bottom water decreased by a factor of 3 compared to the WD and WW seasons. However, the reservoir overturn increased the average CH<sub>4</sub> concentrations in the epilimnion by a factor of 2 ( $3.4 \pm 14.8 \mu\text{mol L}^{-1}$ ) in comparison with the WD and WW seasons. After the commissioning, the CH<sub>4</sub> vertical profiles of concentration before turbine intake (RES9) were homogeneous from the surface to the bottom. The highest average CH<sub>4</sub> concentration from the surface to the bottom peaked up to  $215 \mu\text{mol L}^{-1}$  in July 2010 at this station. On a seasonal basis, the CH<sub>4</sub> concentration at RES9 averaged  $39.8 \pm 48.8$ ,  $29.9 \pm 55.4$ , and  $1.9 \pm 4.3 \mu\text{mol L}^{-1}$  during the WD, WW, and CD seasons, respectively (Fig. 3). The concentrations at RES9 were up to 10 times lower than the maximum bottom concentrations at the other stations for a given season. Since station RES9 behaved differently from the other stations, results from this station will be treated separately.

The overall bottom CH<sub>4</sub> concentration (Fig. 4c) and dissolved CH<sub>4</sub> stock in the reservoir (Fig. 4d) increased at the beginning of the WD season. The higher bottom CH<sub>4</sub> concentration and storage in the reservoir are concomitant with the establishment of anoxia in the hypolimnion and thermal stratification (Fig. 4). Hypolimnetic CH<sub>4</sub> concentration and storage reached their maxima (up to  $508 \pm 254 \mu\text{mol L}^{-1}$  and  $4.7 \pm 0.5 \text{Gg}(\text{CH}_4)$ , Fig. 4c, d) at the end of the WD/beginning of the WW season, when the residence time of water in the reservoir was the lowest (40 days, Fig. 4d) and when the reservoir volume was the smallest (Fig. 2b). Along the WW season, the thermal stratification weakened (Fig. 4a) and the CH<sub>4</sub> concentration and dissolved CH<sub>4</sub> stock decreased (Fig. 4c, d), while the residence time of water increased (Fig. 4d) and the water volume increased (Fig. 2b). In the CD season, the reservoir overturns, as evidenced by the low  $\Delta T$  and the penetration of O<sub>2</sub> into the hypolimnion (Fig. 4a, b). During the CD season, the bottom CH<sub>4</sub> concentration and the storage reached their minima (down to  $1.3 \pm 4.5 \mu\text{mol L}^{-1}$  and  $0.01 \pm 0.001 \text{Gg}(\text{CH}_4)$ , Fig. 4c, d), when the residence time of water was the longest (Fig. 4d). The sharp decrease in CH<sub>4</sub> storage and concentration in the transition from the WW to CD seasons is concomitant with

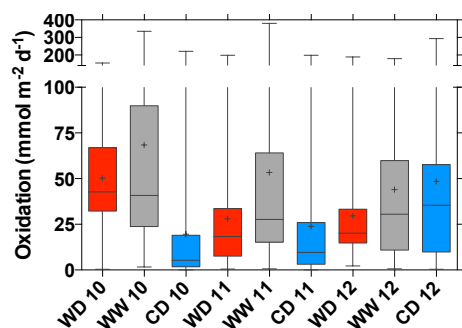


**Figure 5.** Seasonal variations between 2010 and 2012 of the depth-integrated aerobic CH<sub>4</sub> oxidation ( $\text{mmol m}^{-2} \text{d}^{-1}$ ) at stations RES1–RES8 calculated from the aerobic oxidation rates determined by Deshmukh et al. (2016). WD stands for warm dry (in red), WW for warm wet (in grey), and CD for cool dry (in blue). The boxes show the median and the interquartile range, the whiskers denote the full range of values, and the plus sign (+) denotes the mean.

a sharp increase in O<sub>2</sub> concentration at the bottom (up to  $160 \pm 89 \mu\text{mol L}^{-1}$ , Fig. 4).

During the 3.5 years of monitoring, the same seasonal pattern as described above is observed, although the annual CH<sub>4</sub> bottom concentration and storage were threefold higher in 2009 and 2010 than in the year 2011 (Fig. 4c, d). In the dry year 2012, the reservoir bottom CH<sub>4</sub> concentration and storage were almost twice as high as in the wet year 2011.

### 3.3 Aerobic CH<sub>4</sub> oxidation in the reservoir

Between 2010 and 2012, the depth-integrated aerobic CH<sub>4</sub> oxidation rates ranged between 0.05 and  $380 \text{ mmol m}^{-2} \text{d}^{-1}$  at stations RES1–RES8 (Fig. 5). On average, aerobic oxidation was higher in the WW season ( $55 \pm 63 \text{ mmol m}^{-2} \text{d}^{-1}$ ) than in the CD ( $30 \pm 46 \text{ mmol m}^{-2} \text{d}^{-1}$ ) and WD ( $36 \pm 32 \text{ mmol m}^{-2} \text{d}^{-1}$ ) seasons, and it was not statistically different for the 3 years. In the WD season, aerobic CH<sub>4</sub> oxidation was on average twice as high in 2010 than for the following 2 years. In the CD season of the year 2012, the aerobic oxidation rates were exceptionally high compared to the same season in the previous years.

### 3.4 Spatial and seasonal variability of surface CH<sub>4</sub> concentration and diffusive fluxes at the reservoir surface (RES1–RES8)

The surface concentrations at stations RES1–8 ranged from 0.02 to  $150 \mu\text{mol L}^{-1}$  and were  $2.0 \pm 10.5 \mu\text{mol L}^{-1}$  (median = 0.9),  $1.5 \pm 5.5 \mu\text{mol L}^{-1}$  (median = 0.4), and  $3.4 \pm 14.7 \mu\text{mol L}^{-1}$  (median = 0.2) on average for the CD, WD, and WW seasons, respectively. The surface concentration followed a log-logistic distribution, which indicates the existence of extremely high values. This is confirmed by the fact that the skewness of the time series of the log of the CH<sub>4</sub> concentrations for all stations is positive (Fig. S2), especially

at stations RES1, RES3, and RES7, for which the skewness is  $> 1$  (Fig. S2). Over the course of the 3.5 years of survey, the surface concentrations were not statistically different between all stations, and no statistically significant seasonal variations were observed because of the occurrence of sporadic events in all seasons (Fig. S3a). The normalized distribution of concentrations (in log) according to seasons (Fig. 6) indicates that these high concentrations were observed without any clear seasonal trend at stations RES1, RES5, and RES6 ( $< 1$  up to  $150 \mu\text{mol L}^{-1}$ ). At stations RES2 and RES3, the concentrations up to  $128 \mu\text{mol L}^{-1}$  were mostly observed in the CD season when the reservoir overturns. At station RES4 located at the Nam Xot and Nam Theun confluence and at stations RES7 and RES8, both located in the inflow region of the Nam Theun River, the high surface concentrations (up to  $64.60 \mu\text{mol L}^{-1}$ ) were mostly observed during the WW season when the reservoir undergoes sporadic destratification. The auto-correlation function of the time series of the log of the surface CH<sub>4</sub> concentrations and diffusive fluxes at stations RES1–8 indicated that all stations (except RES1) have a memory effect of 30 to 40 days (Fig. S4). This implies that with a sampling frequency of 15 days, we captured most of the changes in the surface CH<sub>4</sub> concentrations. At station RES1, a frequency higher than 15 days would have been better suited since the changes in CH<sub>4</sub> concentrations are faster than at other stations.

During the monitoring at the RES1–RES8 stations, the average diffusive flux was  $2.8 \pm 12.2 \text{ mmol m}^{-2} \text{d}^{-1}$ , ranging from 0.01 to  $201.86 \text{ mmol m}^{-2} \text{d}^{-1}$  without any clear inter-annual and seasonal trends (Fig. S3b). As for the concentrations, flux data followed a log-logistic distribution. The median flux in the WD season is 40 to 80 % higher than the median in the WW and CD seasons, respectively. During the WW and CD seasons, more than 60 % of the calculated fluxes were lower than  $1 \text{ mmol m}^{-2} \text{d}^{-1}$ , which corresponds to a classical flux in pristine rivers. However, the average fluxes in the WW and CD seasons are 30 % higher than in the WD season (Table 2). This confirms the presence of extremely high values during the WD and CD seasons, as expected from the surface concentrations. All seasons together, around 7 % of the diffusive fluxes that we observed were higher than  $5 \text{ mmol m}^{-2} \text{d}^{-1}$ , which corresponds to extremely high diffusive fluxes in comparison with data from the literature for reservoirs and lakes (Bastviken et al., 2008; Barros et al., 2011). The median and average of these extreme fluxes higher than  $5 \text{ mmol m}^{-2} \text{d}^{-1}$  were 2 times higher in the WW and CD seasons than in the WD season (Table 2).

At the NT2R, diffusive CH<sub>4</sub> fluxes covered the whole range of fluxes reported for tropical reservoirs, depending on the season. Most of the fluxes at the NT2R were around 1 order of magnitude lower than those at Petit Saut Reservoir (French Guiana) just after the impoundment (Galy-Lacaux et al., 1997), and of the same order of magnitude as reported for reservoirs 10 to 18 years older (Abril et al., 2005; Guérin et



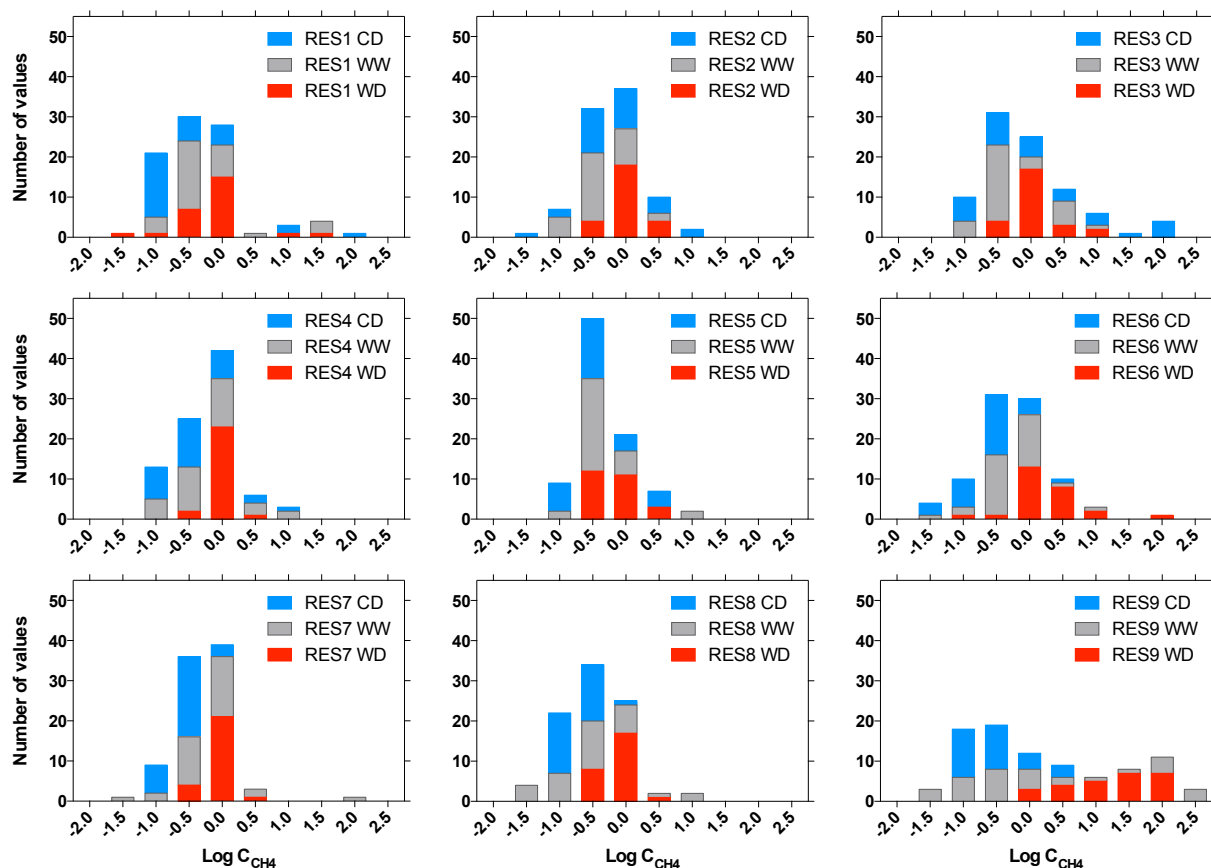


**Figure 6.** Frequency distribution of the log of CH<sub>4</sub> concentrations ( $\mu\text{mol L}^{-1}$ ) at the nine monitoring stations of the Nam Theun 2 Reservoir. The red, grey, and blue colours indicate the warm dry (WD), warm wet (WW), and cool dry (CD) seasons, respectively.

**Table 2.** Median, average, ranges, and proportion of diffusive fluxes ( $F_{\text{CH}_4}$ ) < 1 and > 5  $\text{mmol m}^{-1} \text{d}^{-1}$  for three seasons.

Station	Warm dry (WD)	Warm wet (WW)	Cool dry (CD)
RES1–RES8			
<i>n</i>	212	252	217
Range	0.01–102.59	0.01–201.86	0.01–94.64
Median	1.08	0.64	0.20
Average $\pm$ SD	$2.23 \pm 7.37$	$3.12 \pm 14.58$	$3.04 \pm 12.89$
% $F_{\text{CH}_4} < 1$	48 %	63 %	86 %
% $F_{\text{CH}_4} > 5$	6.6 %	7.5 %	7.4 %
Median $F > 5$	10.67	13.80	23.75
Average $F > 5$	$16.69 \pm 25.04$	$30.23 \pm 45.99$	$36.45 \pm 33.19$
RES9			
<i>n</i>	39	45	36
Range	0.24–342.00	0.03–605.38	0.07–17.62
Median	40.81	1.23	0.48
Average $\pm$ SD	$83.33 \pm 15.57$	$78.58 \pm 24.73$	$2.21 \pm 0.69$

al., 2006; Kemenes et al., 2007; Chanudet et al., 2011). However, some diffusive fluxes at stations RES1–8 in the WW and CD seasons (up to  $202 \text{ mmol m}^{-2} \text{d}^{-1}$ ) are among the highest ever reported at the surface of a hydroelectric reservoir or a lake (Bastviken et al., 2011; Barros et al., 2011) and

rivers downstream of dams (Abril et al., 2005; Guérin et al., 2006; Deshmukh et al., 2016).

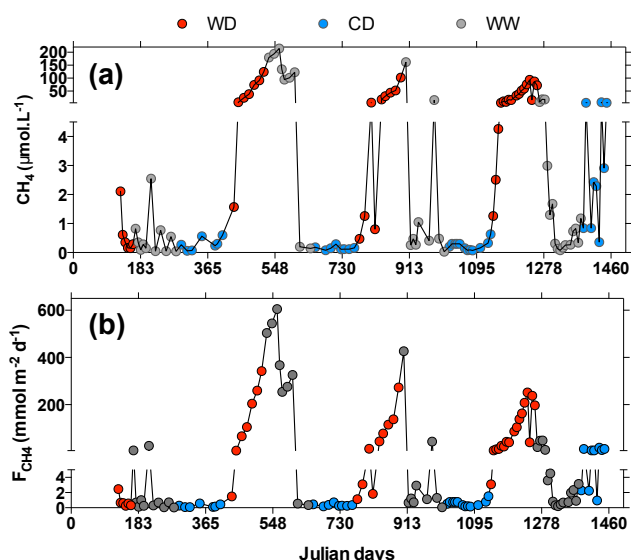


**Figure 7.** (a) Surface concentrations and (b) diffusive fluxes between June 2009 and December 2012 at station RES9 located at the water intake. Julian day 0 is 1 January 2009. The red, grey, and blue colours indicate the warm dry (WD), warm wet (WW), and cool dry (CD) seasons, respectively.

### 3.5 Surface methane concentrations and diffusive fluxes at the water intake (RES9)

Following the commissioning of the reservoir and powering of the turbines (Julian day 450), the CH<sub>4</sub> concentrations at station RES9 (Fig. 7a) located at the water intake were up to 30 times higher than at any other stations. On average, CH<sub>4</sub> concentrations were  $36.6 \pm 35.8 \mu\text{mol L}^{-1}$  (median = 24.3),  $37.6 \pm 67.0 \mu\text{mol L}^{-1}$  (median = 0.9), and  $1.0 \pm 1.7 \mu\text{mol L}^{-1}$  (median = 0.3) in the WD, WW, and CD seasons, respectively. The surface concentrations at RES9 were significantly higher in the WD and WW seasons than in the CD season ( $p = 0.0002$  and Fig. 7a). The highest concentration was observed each year at the end of the WD season/beginning of the WW season in between June and August. These maxima decreased from  $215 \mu\text{mol L}^{-1}$  in August 2010 to  $87 \mu\text{mol L}^{-1}$  in June 2012.

The diffusive fluxes ranged between 0.03 and  $605.38 \text{ mmol m}^{-2} \text{ d}^{-1}$  (Fig. 7b and Table 2). On average, the CH<sub>4</sub> diffusive fluxes at RES9 were 2 to 40 times higher than at the other stations in the CD, WD, and WW seasons. Diffusive fluxes at this station are usually higher than  $10 \text{ mmol m}^{-2} \text{ d}^{-1}$  from April to July, which corresponds to the WD season and the very beginning of the WW season. In 2010, diffusive fluxes were on average  $241 \pm 219$  and  $239 \pm 228 \text{ mmol m}^{-2} \text{ d}^{-1}$ , respectively, for the WD and WW seasons. In 2011 and 2012, the fluxes dropped down by a factor of 2 in the WD season ( $112 \pm 110 \text{ mmol m}^{-2} \text{ d}^{-1}$ ) and almost by a factor of 40 in the WW season ( $6.8 \pm 14.4 \text{ mmol m}^{-2} \text{ d}^{-1}$ ). Overall,

emissions at RES9 decreased by a factor of 2 between 2010 and 2012.

## 4 Discussion

### 4.1 CH<sub>4</sub> dynamic in the reservoir water column

The gradual decrease in the CH<sub>4</sub> concentration from the anoxic bottom water column to the metalimnion and the sharp decrease around the oxicleine in the metalimnion (Fig. 3) is typical in reservoirs and lakes where CH<sub>4</sub> is produced in anoxic sediments and flooded soils (Guérin et al., 2008; Sobek et al., 2012; Maeck et al., 2013), and where most of it is oxidized at the oxic–anoxic interface (Bedard and Knowles, 1997; Bastviken et al., 2002; Guérin and Abril, 2007; Deshmukh et al., 2016).

CH<sub>4</sub> concentrations and storage increase concomitantly with the surface water temperature and the establishment of the thermal stratification during the WD season and peak at the end of the WD season/beginning of the WW season, when the surface and volume of the reservoir were minimum (Figs. 2, 3, and 4). The fact that the storage reached its maximum when the reservoir volume is at its minimum shows that the increase in concentration at the bottom of the reservoir is highly significant. During the WW season, CH<sub>4</sub> concentrations and storage decrease slowly (Fig. 4), while aerobic methane oxidation reaches its maximum (Fig. 5). When the reservoir overturns at the beginning of the CD season, the CH<sub>4</sub> hypolimnetic concentrations and storage reach their minima (Fig. 4). The overturn favours the penetration of oxygen down to the bottom (Figs. 3 and 4b). The sharp decrease in the CH<sub>4</sub> concentrations and CH<sub>4</sub> storage during this period is expected to result from sudden outgassing (Sect. 4.2) together with an enhancement of the aerobic CH<sub>4</sub> oxidation as observed in lakes that overturn (Utsumi et al., a, b; Kankaala et al., 2007; López Bellido et al., 2009; Schubert et al., 2010, 2012; Fernández et al., 2014). A significant increase in methane oxidation during overturn in the CD season was not observed, except for the year 2012 (Fig. 5) when hypolimnetic CH<sub>4</sub> concentrations were still quite high (Fig. 4c, d). The absence of a clear enhancement of the CH<sub>4</sub> oxidation in the water column of NT2R can be attributed to the slow erosion of the thermal stratification before the reservoir really overturns.

As the reservoir overturns during the period over which the water residence time is the longest, the temporal evolution of the concentrations is anti-correlated with the residence time (Fig. 4c, d). The seasonal dynamics of the CH<sub>4</sub> in the monomictic NT2R differs from permanently stratified reservoirs like Petit Saut Reservoir, where CH<sub>4</sub> concentration increased with retention time (Abril et al., 2005). However, at the annual scale the water residence time has a strong influence on CH<sub>4</sub> concentration and storage in the reservoir. Before the reservoir was commissioned (April 2010), the water res-

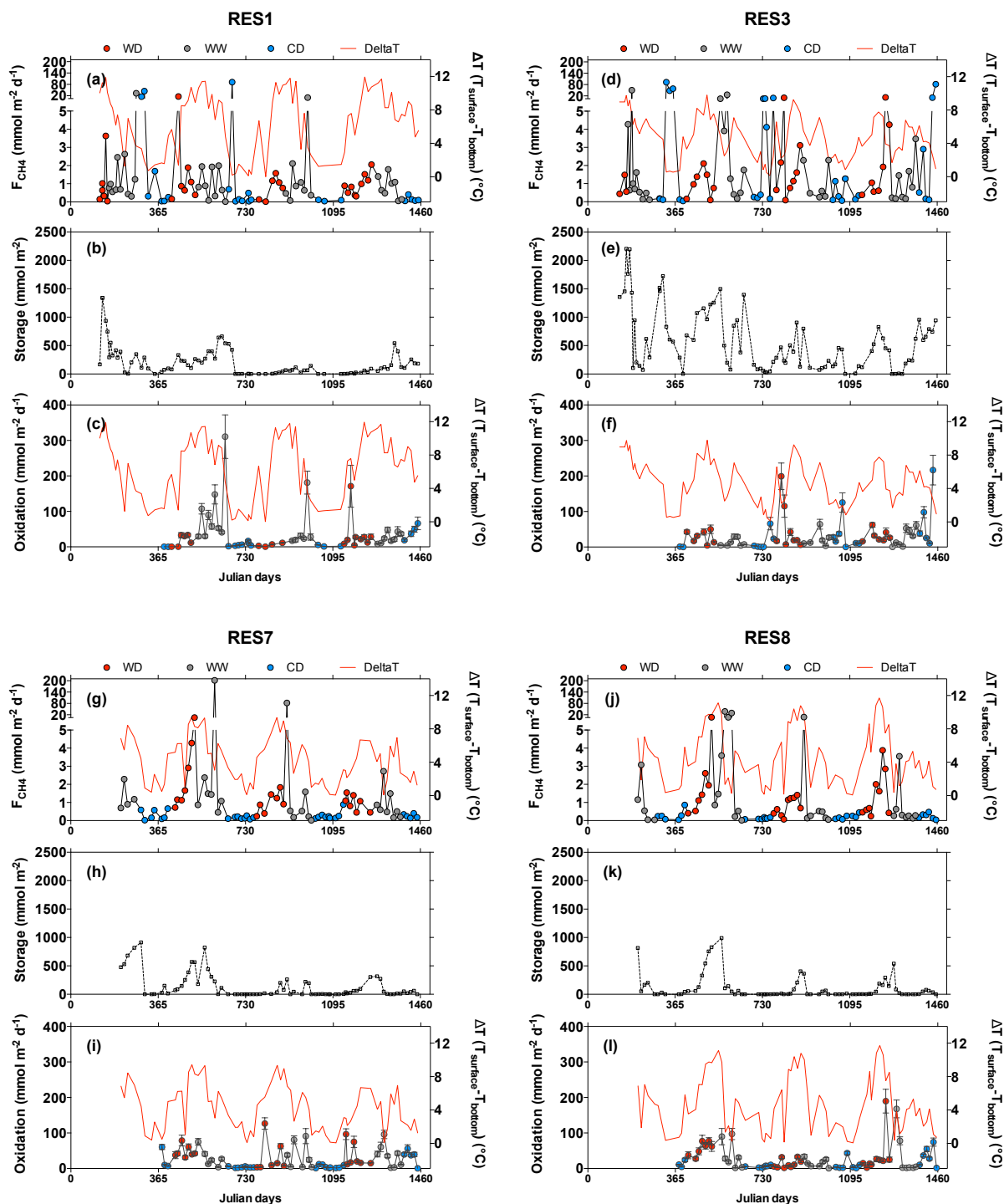


**Figure 8.** (a, d, g, j) Stratification index ( $\Delta T$ , red line; see text) and diffusive fluxes; (b, e, h, k) CH<sub>4</sub> storage and (c, f, i, l) depth-integrated aerobic CH<sub>4</sub> oxidation ( $mmol\ m^{-2}\ d^{-1}$ , black line) calculated from the aerobic oxidation rates determined by Deshmukh et al. (2016) and  $\Delta T$  (red line) between June 2009 and December 2012 at stations RES1, RES3, RES7, and RES8 at the Nam Theun 2 Reservoir. Julian day 0 is 1 January 2009. The red, grey, and blue colour dots indicate the warm dry (WD), warm wet (WW), and cold dry (CD) seasons, respectively.

idence time was up to 4 years and the CH<sub>4</sub> storage was up to 4 times higher than in 2011 and 2012 (Fig. 4d). Although a decrease in concentration and storage with the age of the

reservoir was expected (Abril et al., 2005), storage in the dry year of 2012 was twice that of the wet year of 2011, likely due to a 25 % increase in residence time between 2011 and

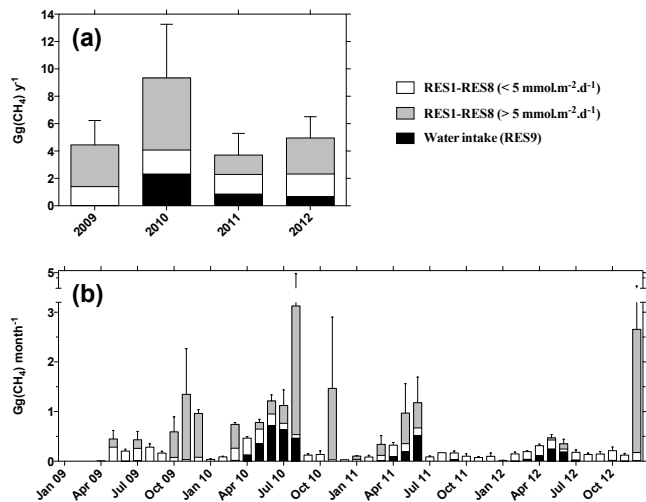


**Figure 9.** (a) Total emissions by diffusive fluxes in 2009, 2010, 2011, and 2012, and (b) monthly emissions by diffusive fluxes between May 2009 and December 2012. Emissions from RES9 (water intake) are shown in black, emissions resulting from diffusive fluxes lower than  $5 \text{ mmol m}^{-2} \text{ d}^{-1}$  from stations RES1 to RES8 are shown in white, and emissions resulting from diffusive fluxes higher than  $5 \text{ mmol m}^{-2} \text{ d}^{-1}$  from stations RES1–RES8 are shown in grey.

2012 due to a decrease in rainfall and water inputs. In wet years like 2011, the thermal stratification is weaker than in dry years, since the warming of the epilimnion is less efficient due to (1) lower insulation and cold water inputs from above, and because (2) the high riverine inputs of water alter the stability of the reservoir thermal stratification, as shown by the sharper decrease in the thermal stratification in 2011 than in 2012 illustrated by the decrease in the stratification index ( $\Delta T$ ) (Fig. 4a). As a consequence, the oxygen diffusion to the hypolimnion was higher in 2011 than in 2012 (Fig. 4b) and it enhanced aerobic methane oxidation by 20 % in the water column in the WW season in 2011 as compared to 2012 (Fig. 5). Therefore our results suggest that the hydrology affects both the thermal stratification and therefore the diffusion of O<sub>2</sub> in the water column. The enhancement of O<sub>2</sub> penetration in rainy years favours the CH<sub>4</sub> oxidation and therefore contributes to the CH<sub>4</sub> storage reduction. With less CH<sub>4</sub> in the water column, the potentiality for downstream emissions (Deshmukh et al., 2016) and emissions through hotspots and hot moments (see below) is highly reduced.

#### 4.2 Hot moments of emissions during sporadic destratification and reservoir overturn

Figure 8 illustrates the evolution of the diffusive fluxes, the stratification index ( $\Delta T$ ), the CH<sub>4</sub> storage, and the aerobic CH<sub>4</sub> oxidation at stations RES1, RES3, RES7, and RES8. These four stations were selected for their contrasting skewness (Fig. S2) which gives an indication of the occurrence of extreme events and the facts that they are representative of all

station characteristics (Table 1). It shows that the large bursts of CH<sub>4</sub> (from 5 up to  $200 \text{ mmol m}^{-2} \text{ d}^{-1}$ ) always occurred in both the CD and WW seasons only when  $\Delta T$  decreased sharply ( $> 4^\circ \text{C}$ , Fig. 8a, d, g, j) and were usually followed by a sharp decrease in the CH<sub>4</sub> storage in the water column (Fig. 8b, e, h, k).

Hot moments of emissions occurred during overturn in the CD at stations RES1 and RES3 as illustrated in Fig. 7. We therefore confirm the occurrence of hot moments of emissions during the reservoir overturn in the CD season as already observed in lakes that overturn in temperate regions (Kankaala et al., 2007; López Bellido et al., 2009; Schubert et al., 2010, 2012; Fernández et al., 2014). The highest emissions determined at the NT2R are 1 order of magnitude higher than previously reported outgassing during overturn and they occur mostly in the section of the reservoir that has the longest water residence time (RES1–3, Table 1) and the largest CH<sub>4</sub> storage (Fig. 8b, e, h, k). This suggests that the impact of reservoir overturn can be very critical for the whole-reservoir CH<sub>4</sub> budget in tropical hydroelectric reservoirs and especially in young ones where hypolimnic concentration could reach up to  $1000 \mu\text{mol L}^{-1}$ .

Hot moments of emissions also occur during sporadic destratifications in the WW season in the inflow region (RES4 and RES6–8) where the inflow of cool water from the watershed might disrupt the thermal stratification in reservoirs (see stations RES7 and 8 in Fig. 8). This is contrast to the observations in reservoirs older than NT2R, where high emissions from the inflow region were recently attributed to an enhancement of CH<sub>4</sub> production fuelled by the sedimentation of organic matter from the watershed (Musenze et al., 2014).

In the WD season, some sporadic emissions occurred, but they were always lower than  $20 \text{ mmol m}^{-2} \text{ d}^{-1}$ , which is up to 10 times lower than extreme fluxes in the WW and CD seasons. Those high fluxes occurred at RES3, RES7, and RES8 (Fig. 8d, g, j) and were associated with  $\Delta T$  variations lower than  $2^\circ \text{C}$ . The CH<sub>4</sub> storage decreases associated with these fluxes, however, were not as sharp as those observed during other seasons (Fig. 8e, h, k). These high emissions were actually associated with early rains and associated high winds that occur sometimes in the last 15 days of May. This shows that a moderate erosion of the stratification when hypolimnic CH<sub>4</sub> concentrations are high could enhance vertical transport of CH<sub>4</sub> toward the surface and emissions into the atmosphere.

Basically, this intense monitoring shows that spatial and temporal variations of CH<sub>4</sub> emissions are largely controlled by the hydrodynamics of the reservoir, with extreme emissions occurring (1) in the inflow region during the wet season and (2) in areas away from the inflow zone during reservoir overturns in the CD season. Even if less frequent, moderate erosion of the stable and steep thermal stratification during warm seasons could also lead to high emissions.

The evolution of depth-integrated aerobic CH<sub>4</sub> oxidation is not clearly related to the reservoir overturns and the CH<sub>4</sub> burst (Fig. 8). Significant increases in the aerobic CH<sub>4</sub> oxidation occurred mostly during the first half of the WD season, when the stratification was unstable, and at the very beginning of the destratification in the WW, when  $\Delta T$  started to decrease. The oxidation could reach high values (up to 380 mmol m<sup>-2</sup> d<sup>-1</sup>) during these two periods since the yield of CH<sub>4</sub> in the water column to sustain the activity of methanotrophs is higher than in the CD season when the reservoir overturns. It shows that in reservoirs or lakes like NT2R that destratify progressively before the overturn, there is no substantial increase in the CH<sub>4</sub> oxidation when the water body finally overturns, as was observed in lakes that overturn within a few days (Kankaala et al., 2007). In addition, the contribution of CH<sub>4</sub> oxidation to the total loss of CH<sub>4</sub> (sum of diffusion and oxidation) in the WD and WW seasons was 90–95 % during the entire monitoring, whereas it was 85 % in the CD season. Therefore, during overturn in the CD season, a significant amount of CH<sub>4</sub> is oxidized, but the removal of CH<sub>4</sub> during overturn is not as efficient as during seasons with a well-established thermal stratification.

During the periods with major loss in the CH<sub>4</sub> storage with concomitant CH<sub>4</sub> burst, we compared the change in the yield of CH<sub>4</sub> with the sum of emissions and oxidation. Most of the time, the emissions alone and/or the sum of emissions and oxidation were significantly higher than the amount of CH<sub>4</sub> that was lost from the water column. At Pääjärvi Lake in Finland (López Bellido et al., 2009), the fact that measured or calculated emissions exceed the loss of CH<sub>4</sub> in the water column was attributed to a probable underestimation of the CH<sub>4</sub> storage in the lake by undersampling the shallow area of the lake. In this study, emissions, storage, and oxidation were estimated at the same stations, avoiding such sampling artefacts. Therefore, it suggests that CH<sub>4</sub> is provided by lateral transport or by production in the flooded soil and biomass (Guérin et al., 2008) at a higher rate than the total loss of CH<sub>4</sub> from the water column by emissions and oxidation. This hypothesis could only be verified by a full CH<sub>4</sub> mass balance including production and total emissions from the reservoir, which is beyond the scope of this article.

#### 4.3 Hotspot of emissions at the water intake (RES9)

After the commissioning of the reservoir, the temperature and the oxygen and CH<sub>4</sub> concentrations were constant from the surface to the bottom of the reservoir at the vicinity of the water intake. On the basis of physical modelling and measurements of water current velocities (Chanudet et al., 2012), the vertical mixing at this station was attributed to the water withdrawal at the intake generating turbulence and water currents over a surface area of 3 km<sup>2</sup>. At this station, CH<sub>4</sub>-rich water from the reservoir hypolimnion reached the surface and led to diffusive fluxes of up to 600 mmol m<sup>-2</sup> d<sup>-1</sup> in the WD–WW seasons (Fig. 7b), whereas fluxes are 3 or-

ders of magnitude lower in the CD season. These high fluxes are the highest reported at the surface of an aquatic ecosystem (Abril et al., 2005; Guérin et al., 2006; Bastviken et al., 2011; Barros et al., 2011; Deshmukh et al., 2016). To the best of our knowledge, this is the first time it is reported that the artificial mixing induced by the water intakes upstream of a dam or a power station enhances emissions significantly. At the NT2R, the intake is located at the bottom of a narrow (130 m) and shallow channel (depth = 9–20 m) on the side of the reservoir (Fig. S1). This design enhances horizontal water current velocities, the vertical mixing, and therefore the emissions. The existence of such a hotspot at other reservoirs might be highly dependant on the design of the water intake (depth among other parameters) and its effect on the hydrodynamics of the reservoir water column.

#### 4.4 Estimation of total diffusive fluxes from the reservoir

Yearly emissions by diffusive fluxes peaked at more than 9 Gg(CH<sub>4</sub>) in 2010 when the reservoir was commissioned, and they decreased to  $\approx 5$  Gg(CH<sub>4</sub>) in 2011 and 2012 (Fig. 9a and Table 3). Yearly integrated at the whole reservoir surface, these emissions correspond to diffusive fluxes of 1.5 to 4 mmol m<sup>-2</sup> d<sup>-1</sup>. These emissions are significantly lower than diffusive fluxes measured at the Petit Saut Reservoir during the first 2 years after flooding, but similar to those determined in the following years (Abril et al., 2005) and values reported for diffusive fluxes from tropical reservoirs in Barros et al. (2011). In the absence of the extreme emissions (both hotspots and hot moments), diffusive emissions from NT2R would have been 1 order of magnitude lower than emissions from tropical reservoirs, as expected from the lower flooded biomass compared to Amazonian reservoirs (Descloux et al., 2011). Due to the specific dynamic of diffusive fluxes at the NT2R with hotspots and hot moments, diffusion at the reservoir surface contributes 18 to 27 % of total emissions (Table 3), which is significantly higher than at other tropical reservoirs where it was measured (see also Deshmukh et al., 2016).

Most of the increase in CH<sub>4</sub> emissions by diffusive fluxes from 4 to 9 Gg(CH<sub>4</sub>) between 2009 and 2010 is due to very significant emissions of 2–3 Gg(CH<sub>4</sub>) at the water intake after the commissioning of the reservoir and resulting artificial mixing (Fig. 9a). This increase might be overestimated because we have no measurements between January and April, but this overestimation might be reasonable since those months are usually associated with the lowest emissions of the year (Fig. 9b). After the commissioning, the outgassing of CH<sub>4</sub> was triggered by the artificial mixing generated by the withdrawal of water from the reservoir to the turbines. Although the area under the influence of the water intake is less than 1 % of the total area of the reservoir, emissions at the water intake contributed between 13 and 25 % of total diffusive emissions and 4 to 10 % when consider-

**Table 3.** Methane emissions from the Nam Theun 2 Reservoir between 2009 and 2012.

Gg(CH <sub>4</sub> ) year <sup>-1</sup>	2009	2010	2011	2012
Emission from reservoir				
Diffusion at RES9 only	0.02 ± 0.01	2.33 ± 0.21	0.86 ± 0.12	0.66 ± 0.11
Total diffusion	4.45 ± 1.01	9.34 ± 2.32	3.71 ± 0.81	4.95 ± 1.09
Contribution of RES9 to diffusion (%)	0.4	24.9	23.2	13.3
Ebullition <sup>1</sup>	11.21 ± 0.16	14.39 ± 0.11	14.68 ± 0.10	12.29 ± 0.09
Total emissions from reservoir (ebullition + diffusion at all stations)	15.66 ± 1.02	23.73 ± 2.32	18.39 ± 0.82	17.25 ± 1.09
Contribution of RES9 (%) to total emissions from reservoir	0.1	9.8	4.7	3.8
Total downstream emissions <sup>2</sup>	7.79 ± 0.90	10.73 ± 0.83	2.29 ± 0.41	2.00 ± 0.32
Total emissions (reservoir + downstream)	23.45 ± 1.36	34.46 ± 2.46	20.67 ± 0.92	19.24 ± 1.14
Contribution of diffusion to total emission	19 %	27 %	18 %	26 %
Contribution of RES9 to total (%)	<0.1	6.8	4.2	3.4

<sup>1</sup> Deshmukh et al. (2014). <sup>2</sup> Deshmukh et al. (2016).

ing both ebullition and diffusion, disregarding the year 2009 (Table 3). It is worth noting that emissions at this site are only significant within 3–5 months per year at the end of the WD season/beginning of the WW season when the storage of CH<sub>4</sub> reaches its maximum in the reservoir (Fig. 9b). This new hotspot equals 20 to 40 % of downstream emissions and contributes between 3 and 7 % of total emissions from the NT2R surface when including ebullition and downstream emissions (Table 3 and Deshmukh et al., 2016). Localized perturbation of the hydrodynamics, especially in lakes or reservoirs with CH<sub>4</sub>-rich hypolimnion, can generate hotspots of emissions contributing significantly to the total emissions from a given ecosystem. These hotspots could be found upstream of dams and water intake in reservoirs but also around aeration stations based on air injection or artificial mixing that could be used for improving water quality in water bodies (Wüest et al., 1992).

The contribution of extreme diffusive fluxes (with daily values being >5 up to 200 mmol m<sup>-2</sup> d<sup>-1</sup>) to total emission by diffusion ranges from 30 to 50 % on a yearly basis (Fig. 9a) and from 40 up to 70 % on a monthly basis (Fig. 9b), although these hot moments represent less than 10 % of the observations during the monitoring. In the literature, the statistical distribution of the CH<sub>4</sub> emissions data set always follows heavy-tailed and right skewed distribution like the log-normal, the generalized Pareto distribution (Windsor et al., 1992; Czepiel et al., 1993; Ramos et al., 2006; DelSontro et al., 2011), or log-logistic (this study), which indicates that CH<sub>4</sub> emissions are always characterized by high episodic fluxes. The quantification of emissions thus requires the highest spatial and temporal resolutions in order to capture as many hot moments as possible. At a single station, there is a possibility that we did not catch the peak of emissions, but extreme emission events never lasted more than 2 months (three consecutive sampling dates) and prob-

ably lasted less than 15 days most of the time (Fig. 8). The auto-correlation function of the concentration time series indicates that a minimum sampling frequency of 1 month is required in this monomictic reservoirs for an accurate description of the change in the surface concentrations and estimation of the emissions (Fig. S4). Although a better temporal resolution than 15 days or monthly would probably improve the estimation of CH<sub>4</sub> emissions from this reservoir, a lower temporal resolution could significantly affect (positively or negatively) the emission factors of this reservoir that overturn gradually over several month. Therefore, the monthly frequency defined for this specific reservoir is probably not applicable to every aquatic ecosystem, especially in lakes or reservoirs that overturn within a week or less (Kankaala et al., 2007; López Bellido et al., 2009; Schubert et al., 2012). However, it suggests that quantification of emissions based on two to four campaigns in a year might significantly affect emissions factors and carbon budgets of ecosystems under study.

## 5 Conclusion

The monitoring of CH<sub>4</sub> diffusive emissions every 2 weeks at nine stations revealed complex temporal and spatial variations that could hardly have been characterized by seasonal sampling. The highest emissions occur sporadically during hot moments in the rainy season and when the reservoir overturns. In the rainy season, they mostly occur in the inflow region because the increase in the discharge of cool water from the reservoir tributaries contributes to sporadic thermal destratification. During the reservoir overturn, extreme emissions occur mostly in areas far from inflows and outflows that are supposed to have the highest water residence time. It shows that diffusive emissions can be sporadically as high

as ebullition and that these hot moments could contribute very significantly to the total emissions from natural aquatic ecosystems and reservoirs. Our results suggest that sporadic emissions cannot be integrated properly into the quantification of emissions and establishments of carbon budgets based only on seasonal sampling (two to four campaigns).

We also identified a new hotspot of emissions upstream of the water intake resulting from the artificial destratification of the water column due to horizontal and vertical mixing generated by the water withdrawal. In the case of the NT2R, emissions from this site contribute up to 25 % of total diffusive emissions over less than 1 % of the total reservoir area. We highly recommend measurements of diffusive fluxes around water intakes (immediately upstream of dams, typically) in order to evaluate whether such results can be generalized.

**The Supplement related to this article is available online at doi:10.5194/bg-13-3647-2016-supplement.**

*Acknowledgements.* The authors thank everyone who contributed to the NT2 monitoring programme, especially the Nam Theun 2 Power Company (NTPC) and Electricité de France (EDF) for providing financial, technical, and logistic support. We are also grateful to the Aquatic Environment Laboratory of the Nam Theun 2 Power Company whose shareholders are EDF, Lao Holding State Enterprise, and Electricity Generating Public Company Limited of Thailand. Chandrashekar Deshmukh benefited from a PhD grant from EDF.

Edited by: S. W. A. Naqvi

## References

- Abril, G., Guérin, F., Richard, S., Delmas, R., Galy-Lacaux, C., Gosse, P., Tremblay, A., Varfalvy, L., Dos Santos, M. A., and Matvienko, B.: Carbon dioxide and methane emissions and the carbon budget of a 10-year old tropical reservoir (Petit Saut, French Guiana), *Global Biogeochem. Cy.*, 19, Gb4007, doi:10.1029/2005gb002457, 2005.
- Abril, G., Commarieu, M.-V., and Guérin, F.: Enhanced methane oxidation in an estuarine turbidity maximum, *Limnol. Oceanogr.*, 52, 470–475, 2007.
- Barros, N., Cole, J. J., Tranvik, L. J., Prairie, Y. T., Bastviken, D., Huszar, V. L. M., del Giorgio, P., and Roland, F.: Carbon emission from hydroelectric reservoirs linked to reservoir age and latitude, *Nat. Geosci.*, 4, 593–596, 2011.
- Bastviken, D., Ejlertsson, J., and Tranvik, L.: Measurement of methane oxidation in lakes: A comparison of methods, *Environ. Sci. Technol.*, 36, 3354–3361, doi:10.1021/es010311p, 2002.
- Bastviken, D., Cole, J. J., Pace, M. L., and Van de Bogert, M. C.: Fates of methane from different lake habitats: Connecting whole-lake budgets and CH<sub>4</sub> emissions, *J. Geophys. Res.-Biogeo.*, 113, G02024, doi:10.1029/2007jg000608, 2008.
- Bastviken, D., Tranvik, L. J., Downing, J. A., Crill, P. M., and Enrich-Prast, A.: Freshwater Methane Emissions Offset the Continental Carbon Sink, *Science*, 331, 6013, doi:10.1126/science.1196808, 2011.
- Bedard, C. and Knowles, R.: Some properties of methane oxidation in a thermally stratified lake, *Can. J. Fish. Aquat. Sci.*, 54, 1639–1645, 1997.
- Borges, A. V., Delille, B., Schiettecatte, L. S., Gazeau, F., Abril, G., and Frankignoulle, M.: Gas transfer velocities of CO<sub>2</sub> in three European estuaries (Randers Fjord, Scheldt, and Thames), *Limnol. Oceanogr.*, 49, 1630–1641, 2004.
- Chanudet, V., Descloux, S., Harby, A., Sundt, H., Hansen, B. H., Brakstad, O., Serca, D., and Guérin, F.: Gross CO<sub>2</sub> and CH<sub>4</sub> emissions from the Nam Ngum and Nam Leuk sub-tropical reservoirs in Lao PDR, *Sci. Total Environ.*, 409, 5382–5391, doi:10.1016/j.scitotenv.2011.09.018, 2011.
- Chanudet, V., Fabre, V., and van der Kaaij, T.: Application of a three-dimensional hydrodynamic model to the Nam Theun 2 Reservoir (Lao PDR), *J. Great Lakes Res.*, 38, 260–269, doi:10.1016/j.jglr.2012.01.008, 2012.
- Chen, H., Wu, Y., Yuan, X., Gao, Y., Wu, N., and Zhu, D.: Methane emissions from newly created marshes in the drawdown area of the Three Gorges Reservoir, *J. Geophys. Res.*, 114, D18301, doi:10.1029/2009JD012410, 2009.
- Chen, H., Yuan, X., Chen, Z., Wu, Y., Liu, X., Zhu, D., Wu, N., Zhu, Q. A., Peng, C., and Li, W.: Methane emissions from the surface of the Three Gorges Reservoir, *J. Geophys. Res.*, 116, D21306, doi:10.1029/2011jd016244, 2011.
- Czepiel, P. M., Crill, P. M., and Harriss, R. C.: Methane emissions from municipal wastewater treatment processes, *Environ. Sci. Technol.*, 27, 2472–2477, doi:10.1021/es00048a025, 1993.
- Delignette-Muller, M. L., Dutang, C., Pouillot, R., and Denis, J.-B.: An R Package for Fitting Distributions, <https://cran.r-project.org/web/packages/fitdistrplus/vignettes/paper2JSS.pdf> (last access: 20 June 2016), 1.0–4, 2015.
- DelSontro, T., McGinnis, D. F., Sobek, S., Ostrovsky, I., and Wehrli, B.: Extreme Methane Emissions from a Swiss Hydropower Reservoir: Contribution from Bubbling Sediments, *Environ. Sci. Technol.*, 44, 2419–2425, doi:10.1021/es9031369, 2010.
- DelSontro, T., Kunz, M. J., Kemper, T., Wüest, A., Wehrli, B., and Senn, D. B.: Spatial Heterogeneity of Methane Ebullition in a Large Tropical Reservoir, *Environ. Sci. Technol.*, 45, 9866–9873, doi:10.1021/es2005545, 2011.
- Descloux, S., Chanudet, V., Poilvé, H., and Grégoire, A.: Co-assessment of biomass and soil organic carbon stocks in a future reservoir area located in Southeast Asia, *Environ. Monit. Assess.*, 173, 723–741, doi:10.1007/s10661-010-1418-3, 2011.
- Descloux, S., Guedant, P., Phommachanh, D., and Luthi, R.: Main features of the Nam Theun 2 hydroelectric project (Lao PDR) and the associated environmental monitoring programmes, *Hydroécol. Appl.*, 19, 5–25, 2016.
- Deshmukh, C., Serça, D., Delon, C., Tardif, R., Demarty, M., Jarnot, C., Meyerfeld, Y., Chanudet, V., Guédant, P., Rode, W., Descloux, S., and Guérin, F.: Physical controls on CH<sub>4</sub> emissions from a newly flooded subtropical freshwater hydroelectric reservoir: Nam Theun 2, *Biogeosciences*, 11, 4251–4269, doi:10.5194/bg-11-4251-2014, 2014.
- Deshmukh, C., Guérin, F., Labat, D., Pighini, S., Vongkhamsoo, A., Guédant, P., Rode, W., Godon, A., Chanudet, V., Descloux, S.,

- and Serça, D.: Low methane (CH<sub>4</sub>) emissions downstream of a monomictic subtropical hydroelectric reservoir (Nam Theun 2, Lao PDR), *Biogeosciences*, 13, 1919–1932, doi:10.5194/bg-13-1919-2016, 2016.
- Dumestre, J. F., Guezennec, J., Galy-Lacaux, C., Delmas, R., Richard, S., and Labroue, L.: Influence of Light Intensity on Methanotrophic Bacterial Activity in Petit Saut Reservoir, French Guiana, *Appl. Environ. Microb.*, 65, 534–539, 1999.
- Fernández, J. E., Peeters, F., and Hofmann, H.: Importance of the Autumn Overturn and Anoxic Conditions in the Hypolimnion for the Annual Methane Emissions from a Temperate Lake, *Environ. Sci. Technol.*, 48, 7297–7304, doi:10.1021/es4056164, 2014.
- Galy-Lacaux, C., Delmas, R., Jambert, C., Dumestre, J. F., Labroue, L., Richard, S., and Gosse, P.: Gaseous emissions and oxygen consumption in hydroelectric dams: A case study in French Guyana, *Global Biogeochem. Cy.*, 11, 471–483, 1997.
- Gross, J. and Ligges, U.: Tests for Normality (Nortest), <https://cran.r-project.org/web/packages/nortest/nortest.pdf> (last access: 20 June 2016), 1.04-4, 2015.
- Guérin, F. and Abril, G.: Significance of pelagic aerobic methane oxidation in the methane and carbon budget of a tropical reservoir, *J. Geophys. Res.-Biogeo.*, 112, G03006, doi:10.1029/2006jg000393, 2007.
- Guérin, F., Abril, G., Richard, S., Burban, B., Reynouard, C., Seyler, P., and Delmas, R.: Methane and carbon dioxide emissions from tropical reservoirs: Significance of downstream rivers, *Geophys. Res. Lett.*, 33, L21407, doi:10.1029/2006gl027929, 2006.
- Guérin, F., Abril, G., Serça, D., Delon, C., Richard, S., Delmas, R., Tremblay, A., and Varfalvy, L.: Gas transfer velocities of CO<sub>2</sub> and CH<sub>4</sub> in a tropical reservoir and its river downstream, *J. Marine Syst.*, 66, 161–172, doi:10.1016/j.jmarsys.2006.03.019, 2007.
- Guérin, F., Abril, G., de Junet, A., and Bonnet, M.-P.: Anaerobic decomposition of tropical soils and plant material: Implication for the CO<sub>2</sub> and CH<sub>4</sub> budget of the Petit Saut Reservoir, *Appl. Geochem.*, 23, 2272–2283, doi:10.1016/j.apgeochem.2008.04.001, 2008.
- Jahne, B., Munnich, K. O., Bosinger, R., Dutzi, A., Huber, W., and Libner, P.: On the parameters influencing air-water gas-exchange, *J. Geophys. Res.-Oceans*, 92, 1937–1949, 1987.
- Kankaala, P., Taipale, S., Nykanen, H., and Jones, R. I.: Oxidation, efflux, and isotopic fractionation of methane during autumnal turnover in a polyhumic, boreal lake, *J. Geophys. Res.-Biogeo.*, 112, G02003, doi:10.1029/2006jg000336, 2007.
- Kemenes, A., Forsberg, B. R., and Melack, J. M.: Methane release below a tropical hydroelectric dam, *Geophys. Res. Lett.*, 34, L12809, doi:10.1029/2007gl029479, 2007.
- López Bellido, J., Tulonen, T., Kankaala, P., and Ojala, A.: CO<sub>2</sub> and CH<sub>4</sub> fluxes during spring and autumn mixing periods in a boreal lake (Pääjärvi, southern Finland), *J. Geophys. Res.-Biogeo.*, 114, G04007, doi:10.1029/2009JG000923, 2009.
- MacIntyre, S., Jonsson, A., Jansson, M., Aberg, J., Turney, D. E., and Miller, S. D.: Buoyancy flux, turbulence, and the gas transfer coefficient in a stratified lake, *Geophys. Res. Lett.*, 37, L24604, doi:10.1029/2010GL044164, 2010.
- Maeck, A., DelSontro, T., McGinnis, D. F., Fischer, H., Flury, S., Schmidt, M., Fietzek, P., and Lorke, A.: Sediment Trapping by Dams Creates Methane Emission Hot Spots, *Environ. Sci. Technol.*, 47, 8130–8137, doi:10.1021/es4003907, 2013.
- McClain, M. E., Boyer, E. W., Dent, C. L., Gergel, S. E., Grimm, N. B., Groffman, P. M., Hart, S. C., Harvey, J. W., Johnston, C. A., Mayorga, E., McDowell, W. H., and Pinay, G.: Biogeochemical hot spots and hot moments at the interface of terrestrial and aquatic ecosystems, *Ecosystems*, 6, 301–312, doi:10.1007/s10021-003-0161-9, 2003.
- Musenze, R. S., Grinham, A., Werner, U., Gale, D., Sturm, K., Udy, J., and Yuan, Z.: Assessing the Spatial and Temporal Variability of Diffusive Methane and Nitrous Oxide Emissions from Subtropical Freshwater Reservoirs, *Environ. Sci. Technol.*, 48, 14499–14507, doi:10.1021/es505324h, 2014.
- NTPC: Environmental Assessment and Management Plan – Nam Theun 2 Hydroelectric Project. Nam Theun 2 Power Company, NTPC (Nam Theun 2 Power Company), Vientiane, 212, 2005.
- Pacheco, F. S., Soares, M. C. S., Assireu, A. T., Curtarelli, M. P., Roland, F., Abril, G., Stech, J. L., Alvalá, P. C., and Ometto, J. P.: The effects of river inflow and retention time on the spatial heterogeneity of chlorophyll and water-air CO<sub>2</sub> fluxes in a tropical hydropower reservoir, *Biogeosciences*, 12, 147–162, doi:10.5194/bg-12-147-2015, 2015.
- R Development Core Team: R: A Language and Environment for Statistical Computing, R Foundation for Statistical Computing, Vienna, Austria, 3-900051-07-0, 2008.
- Ramos, F. M., Lima, I. B. T., Rosa, R. R., Mazzi, E. A., Carvalho, J. O. C., Rasera, M. F. F. L., Ometto, J. P. H. B., Assireu, A. T., and Stech, J. L.: Extreme event dynamics in methane ebullition fluxes from tropical reservoirs, *Geophys. Res. Lett.*, 33, L21404, doi:10.1029/2006gl027943, 2006.
- Schubert, C., Lucas, F., Durisch-Kaiser, E., Stierli, R., Diem, T., Scheidegger, O., Vazquez, F., and Müller, B.: Oxidation and emission of methane in a monomictic lake (Rotsee, Switzerland), *Aquat. Sci.*, 72, 455–466, doi:10.1007/s00027-010-0148-5, 2010.
- Schubert, C. J., Diem, T., and Eugster, W.: Methane Emissions from a Small Wind Shielded Lake Determined by Eddy Covariance, Flux Chambers, Anchored Funnels, and Boundary Model Calculations: A Comparison, *Environ. Sci. Technol.*, 46, 4515–4522, doi:10.1021/es203465x, 2012.
- Sobek, S., DelSontro, T., Wongfun, N., and Wehrli, B.: Extreme organic carbon burial fuels intense methane bubbling in a temperate reservoir, *Geophys. Res. Lett.*, 39, L01401, doi:10.1029/2011gl050144, 2012.
- St Louis, V. L., Kelly, C. A., Duchemin, E., Rudd, J. W. M., and Rosenberg, D. M.: Reservoir surfaces as sources of greenhouse gases to the atmosphere: A global estimate, *Bioscience*, 50, 766–775, 2000.
- Sturm, K., Yuan, Z., Gibbes, B., Werner, U., and Grinham, A.: Methane and nitrous oxide sources and emissions in a subtropical freshwater reservoir, South East Queensland, Australia, *Biogeosciences*, 11, 5245–5258, doi:10.5194/bg-11-5245-2014, 2014.
- Teodoru, C. R., Bastien, J., Bonneville, M.-C., del Giorgio, P. A., Demarty, M., Garneau, M., Hélie, J.-F., Pelletier, L., Prairie, Y. T., Roulet, N. T., Strachan, I. B., and Tremblay, A.: The net carbon footprint of a newly created boreal hydroelectric reservoir, *Global Biogeochem. Cy.*, 26, GB2016, doi:10.1029/2011gb004187, 2012.
- Utsumi, M., Nojiri, Y., Nakamura, T., Nozawa, T., Otsuki, A., and Seki, H.: Oxidation of dissolved methane in a eutrophic, shallow



- lake: Lake Kasumigaura, Japan, *Limnol. Oceanogr.*, 43, 471–480, 1998a.
- Utsumi, M., Nojiri, Y., Nakamura, T., Nozawa, T., Otsuki, A., Takamura, N., Watanabe, M., and Seki, H.: Dynamics of dissolved methane and methane oxidation in dimictic Lake Nojiri during winter, *Limnol. Oceanogr.*, 43, 10–17, 1998b.
- Wanninkhof, R.: Relationship between wind-speed and gas-exchange over the ocean, *J. Geophys. Res.-Oceans*, 97, 7373–7382, 1992.
- Windsor, J., Moore, T. R., and Roulet, N. T.: Episodic fluxes of methane from subarctic fens, *Can. J. Soil Sci.*, 72, 441–452, doi:10.4141/cjss92-037, 1992.
- Wüest, A., Brooks, N. H., and Imboden, D. M.: Bubble plume modeling for lake restoration, *Water Resour. Res.*, 28, 3235–3250, doi:10.1029/92WR01681, 1992.
- Yamamoto, S., Alcauskas, J. B., and Crozier, T. E.: Solubility of methane in distilled water and seawater, *J. Chem. Eng. Data*, 21, 78–80, doi:10.1021/jc60068a029, 1976.
- Zheng, H., Zhao, X. J., Zhao, T. Q., Chen, F. L., Xu, W. H., Duan, X. N., Wang, X. K., and Ouyang, Z. Y.: Spatial-temporal variations of methane emissions from the Ertan hydroelectric reservoir in southwest China, *Hydrol. Process.*, 25, 1391–1396, doi:10.1002/hyp.7903, 2011.